Geotechnical and geochemical investigations of the Marquês de Pombal landslide at the Portuguese continental margin

Marion Minning, Dierk Hebbeln, Christian Hensen & Achim Kopf

Minning, M., Hebbeln, D., Hensen, C. & Kopf, A.: Geotechnical and geochemical investigations of the Marquês de pombal landslide at the Portuguese continental margin. *Norwegian Journal of Geology*, Vol. 86x, pp. 187-198. Trondheim 2006, ISSN 029-196X.

The continental slope of the SW Portuguese continental margin is a geomorphologically diverse, tectonically active area with active faulting, canyon formation and mass wasting. Along the Marquês de Pombal fault (MPF), a submarine landslide was geophysically surveyed several years ago. Recently, five sediment cores from different parts of the landslide area were taken near its headwall, along its flow path, and at the distal lobe near the abyssal plain. At these cores, pore water chemistry and sediment physical properties such as index properties, grain size distribution, shear strength and frictional stability were measured. The most interesting results were found near the headwall and at the toe of the slide. The headwall sediment is characterised by low shear strength, high clay content, and an increase in shear strength when shear rate increases; velocity strengthening. The latter is usually expressed by a positive frictional response to a sudden change in sliding velocity (positive [a-b] values). These characteristics are all in favour of triggering slope failure and stable sliding behaviour. In contrast, the sediment at the toe of the slide show largely [a-b] values near zero or even negative, except one layer at 225 cm below seafloor that tends to velocity-strengthen. Interestingly, at this level pore water composition shows a profound deviation in many elements analysed, suggesting that the base of the most proximal portion of the slide was penetrated here. Modelling of geochemical deviation allows us to tentatively estimate deposition of this outermost lobe of remobilised sediment to 5 yrs. BP, which coincides with a regional M4.3 earthquake. We conclude, however, that this age corresponds to minor taper readjustments, while the main landslide event took place much earlier (see Vizcaino et al., this volume).

M. Minning, D. Hebbeln & A. Kopf, RCOM Research Centre Ocean Margins, University of Bremen, Leobener Str., 28359 Bremen, Germany; C. Hensen, IfM-GEOMAR, University of Kiel, Wischhofstr. 1-3, 24148 Kiel, Germany; corresponding author (akopf@uni-bremen.de)

Introduction

The inherent mechanisms and factors governing slope stability and submarine landslides are known because of extensive research carried out by academia and industry, however, the temporal and spatial variability of landslide processes remain poorly understood. In fact, the exact trigger mechanisms of only a few submarine landslides are known with certainty (Mienert et al. 2003). In general, submarine landslides occur due to an increase in loading on a sediment-laden slope, which may in turn lead to an increase in shear stress, or a reduction in shear strength. Possible trigger mechanisms for submarine landslides include sea level change, high sedimentation rates, oversteepening of the slope gradient, wave activity (especially during storm events), gas hydrate dissociation, pore pressure increase, tsunamis, and earthquakes.

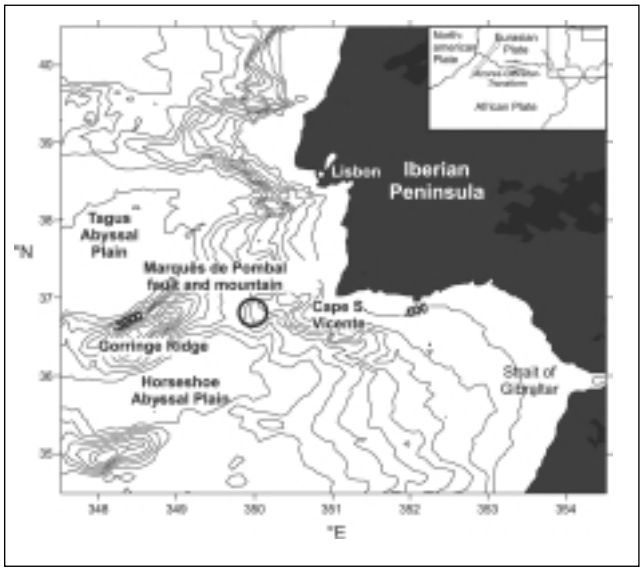

Fig 1: Location of the study area at the Iberian continental margin, southwest of Portugal. Small map in the top right-hand of the map shows the E-W-trending Azores-Gibraltar transform fault.

The region in the eastern North Atlantic southwest of the Iberian Peninsula was selected for this study (Fig. 1), because it comprises a geological setting where the interplay of many of the mentioned processes take place. It hosts the plate boundary between Eurasia and Africa, which is expressed as the Azores-Gibraltar transform fault. Smaller fault zones are located at the continental margin offshore Portugal, one of which is

the steeply-dipping Marquês de Pombal Fault (MPF). Here, a submarine landslide was observed a few years ago (Gràcia et al., 2003). Having been briefed about the location, RV SONNE cruise SO-175 (Kopf et al., 2004) re-visited the area and recovered five sediment cores from the landslide.

In this paper, we present the results from geotechnical and geochemical measurements on five gravity cores taken near the MPF at and adjacent to the landslide. The main focus was dedicated to the geotechnical experiments, which included ring shear tests in addition to the standard measurement of sediment physical properties (density, p-wave velocity, stiffness, grain size distribution, water content). The main objective was to characterise the physical behaviour and frictional stability of the sediments in order to relate them to its potential trigger mechanism.

Geological setting

In our study area, the plate boundary between Eurasia and Africa trends roughly E-W, connecting the Azores-Triple junction to the Gibraltar Strait (e.g., Zitellini et al. 2004). This boundary is a diffuse transpressional plate boundary, called Azores-Gibraltar transform (Sartori et al., 1994). In the area between the Gorringe Ridge and the Strait of Gibraltar, the relative convergence between the two plates is only 4 mm/yr in a NW-SE direction (Argus et al. 1989). The Great Lisbon earthquake of 1755 (e.g. Gutscher 2004) occurred in this region and was one of the largest and most destructive earthquakes with tsunami occurred in historical times in Western Europe.

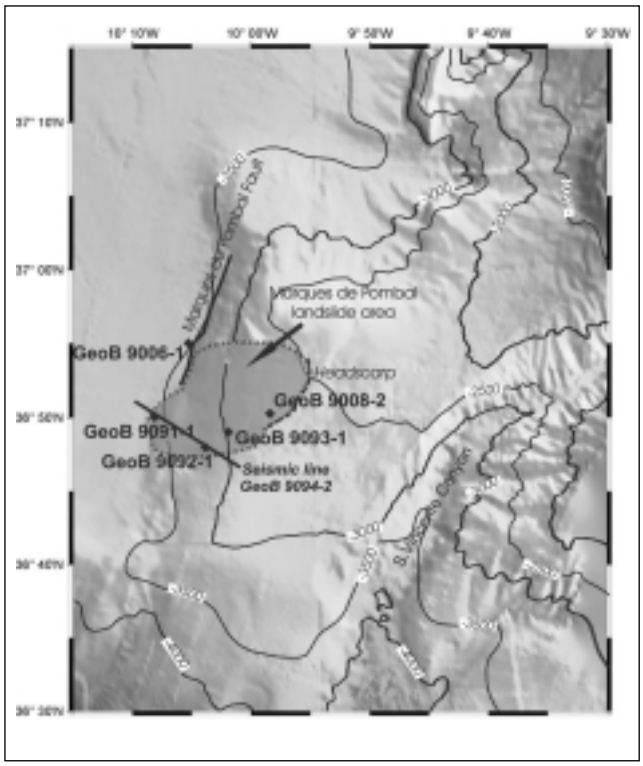

Fig 2: Bathymetric chart of the study area including the approximate location of the landslide and the locations of the investigated sediment cores and the position of the seismic profile. The shaded area shows the approximate area affected by landsliding, whereas the heavy black N-S-trending line shows the trace of the MPF.

The continental slope of the SW Portuguese margin displays two promontories before reaching abyssal depth, one of which is the area of this investigation, the Marquês de Pombal Mountain (Zitellini et al. 2004). A 50 km long suture, the Marquês de Pombal Fault, terminates the western edge of the Marquês de Pombal Mountain (Fig. 1), and exhibits a pronounced N20°E-trending escarpment, which rises about 1 km above the surrounding seafloor. A submarine landslide was observed in its vicinity (Gràcia et al. 2003) (Fig. 2). This landslide consists of two individual parts, a northern and a southern flow (for a detailed description of the slide see Vizcaino et al. this volume). The distance from the up to 25 m high head scarp to the most distal lobe of the southern flow of this slide is about 24 km (approximately EW-direction), whereas the north-south extension is around 11 km. The head scarp is located about 1300 m above the outermost western lobe. According to a geomorphological reconstruction, both the northern and southern flow where directed westward onto the Horseshoe abyssal plain owing to the regional topography. Their laminar nature makes Gràcia and others (this volume) believe the total volume of mobilised sediment does not exceed 1.3 km^3. Given that the MPF and related landslides have also ben discussed in the context of the causes of the 1755 M8.5-9 Lisbon earthquake (Kopf et al. 2004), we assume a much larger sediment mass may have slide in the area of investigation.

During cruise SO-175, the area was geophysically re-surveyed (bathymetry as well as seismic reflection lines; Kopf et al. 2004) and inspected with a deep-towed video system. In addition, four gravity cores and a series of in situ heat flow measurements were taken from the head scarp to the most distal lobe of the southern flow of this landslide, plus a reference core on the adjacent Horseshoe abyssal plain (Table 1 and Fig. 2). In more detail, core GeoB 9008-2 was taken in the head scarp area of the landslide, GeoB 9093-1 and GeoB 9092-1 were taken across the landslide body, GeoB 9091-1 originates from the most distal lobe of the slide, and GeoB 9006-1 was taken for reference.

Methods

We here describe briefly the flow path the gravity cores underwent. Cores were cut into 1m-long sections and

Table 1. Sediment cores taken in the Marquês de Pombal land slide area at the Portuguese continental margin during cruise SO175.

Station no.	latitude °N	longitude °W	water depth (m)	length (m)
GeoB 9006-1	36:55.00'	10:05.56'	3949	4.30
GeoB 9008-2	36:50.29'	09:58.57'	2711	2.68
GeoB 9091-1	36:50.02'	10:08.72'	3921	3.47
GeoB 9092-1	36:47.99'	10:04.00'	3230	4.05
GeoB 9093-1	36:49.03'	10:01.95'	3003	5.20

Table 1. Sediment cores taken in the Marquês de Pombal land slide area at the Portuguese continental margin during cruise SO175.

split on board the ship. They were then photographed and described sedimentologically. Back at RCOM Bremen, the archive half of each core was measured with a non-destructive multi-sensor core logger while discrete specimens from the working half of each core were used for analyses of density/porosity, grain size distribution, and shear strength. Immediately after splitting of the core, some material was taken from the working half to squeeze pore waters. Analyses were largely carried out on board RV Sonne.

Multi-sensor core logging

All cores underwent logging using a GEOTEK Multi Sensor Track (MST) on board RV Sonne prior to splitting. This method allows continuous, nondestructive measurements using the following sensors respectively:

a) Ultrasonic Transducers to measure the velocity of compressional waves in the core (p-wave-velocity).
b) A Gamma Ray Source and Detector for measuring the attenuation of gamma rays through the core (providing density/porosity values).
c) A Magnetic Susceptibility Sensor to determine the amount of magnetically susceptible material present in the sediments.

Physical properties and ring shear tests

Bulk density, grain density and porosity of the samples were measured on ca. 5 cm^3 samples using a Quantachrome Pentapycnometer. The pycnometer measures the volume of the dry sample in a calibrated sample cell. Afterwards, the porosity and density of the sediment can be calculated from the weight and the volume of the samples prior to and after drying.

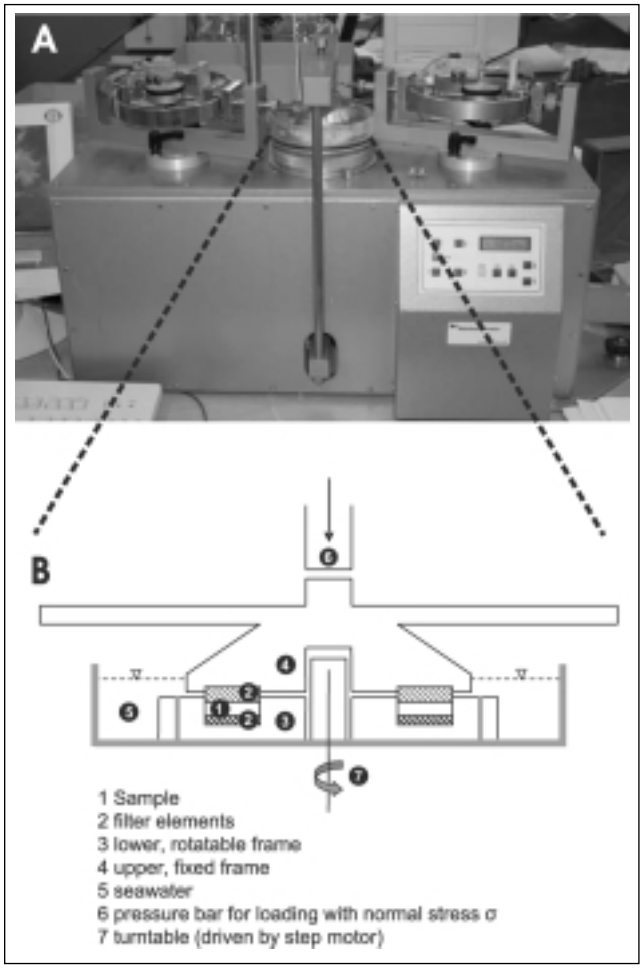

Fig 3: A) Photograph of the Wykeham-Farrance ring shear apparatus at RCOM Bremen; B) Diagram showing principle of the ring shear apparatus.

Grain size measurements were made using a Beckmann-Coulter Laser Particle Sizer LS200. Prior to the analysis, the sample is suspended in demineralised water. It is then continuously pumped through the system, which is scanned by a laser. A number of detectors is collecting the dispersed laser light. Signal intensity is then used to quantify particle size. Sodium pyrophosphate was added to the samples to prevent the formation of aggregates. For all cores samples have been analysed for grain size distribution and porosity in 10 cm intervals.

One of the key parameters in any slope stability study is the strength of the sediment, which we determined in two ways. First, a falling cone penetrometer (Wykeham Farrance WF 21600) was used on the split face of the working half of the core. The weight of the cone is 80,51g and the cone angle is 30°. This method allows a first-order estimate of the sediment stiffness in the (shipboard) laboratory. With its defined weight and geometry, the cone's tip is set onto the split core face, and then released (free drop). Tests were carried out in intervals of five centimetres distance. Hansbo (1957)

made a detailed study of the relationship between the cone penetration and soil strength. According to this work, the undrained shear strength c_u can be calculated from the variables mass *m* and tip angle of the falling cone, the gravity *g*, the penetration *d* and the cone factor *k*. The cone factor is a constant, depending on the angle of the cone and has a value between 0,8 and 1 for a 30° cone (Hansbo 1957). Wood (1985) calculated from fall-cone and miniature vane tests average values of cone factors (k=0,85 for a 30° cone). The undrained shear strength can be calculated from falling cone penetrometer tests using the equation $c_u = (k^*m^*g)/d^2$.

The heart of our analyses was the measurement of peak and residual shear strength as well as frictional stability of the sediment samples using a Bromhead ring shear apparatus manufactured by Wykeham Farrance (see Fig. 3). The sample cell is located between two overlying ring-shaped frames. The sample cell can be submerged in a water-bath during the test. Vertical pressure (i.e., normal stress) can be applied to the sample through the upper porous frame by means of a lever-arm arrangement using hanger weights. Maximum normal stresses of 25 MPa can be reached with the custom-made device at RCOM Bremen. The lower part of the frame is rotable by a motorised drive unit, while the upper part is restrained by the weight via the lever arm as well as a pair of calibrated load rings. Apart from measuring the peak strength during failure, this method allows for quasi-infinite strain on the residual path. Here, velocity stepping tests can be used to determine frictional stability (i.e. stable sliding vs. stick-slip). Details regarding the measuring principle are outlined in Bishop and others (1971).

For each of the cores, we carried out ring shear tests at various normal stresses and sliding velocities. Loading increments were chosen to correspond with the current stress state of the sediments (very little overburden, i.e. 0.25 MPa), and were then increased to 0.5, 1, 2, 4, 8, and finally to a maximum of 16 MPa (i.e. 2000 m of overburden at bulk densities of 2 g/cm^3). The rationale for incrementally submitting the material to higher stresses was to simulate the behaviour of the sediments near the MPF when a thick package is about to slide. Also, high stress experiments provide more reliable results with respect to rate-dependent variations in strength and stability. Our absolute shear strength values are later normalised against normal stress, where the coefficient of friction (μ) is the ratio between shear stress/normal stress.

Our velocity stepping tests were carried out at rates of 0.005, 0.001 and 0.1 mm/s, simulating processes from creep to moderately fast sliding. At each point the shear rate is varied, it is possible to calculate the [a-b]-parameter (see below, and review by Scholz 1998). The [a-b]-value represents the frictional response to a suddenly imposed increase or decrease in sliding velocity. The [a-b]-value is simply calculated from the net change in residual shear strength after increasing or decreasing the sliding velocity. If the residual strength increases with increasing shear rate, an [a-b]-value ≥0 is observed, indicating velocity strengthening behaviour (and stable sliding). If, in contrast, the residual strength decreases when shear rate is risen, the [a-b]-value lies below zero, exhibiting velocity weakening and potentially unstable behaviour and stick-slip. Clay minerals generally show stable sliding and velocity strengthening behaviour, at least when water-saturated (e.g. Kopf & Brown 2003). Mechanically stronger components such as quartzitic silt and sand particles tend to velocity weaken the sediment and may be the reason for unstable deformation (e.g. earthquake rupture).

Pore water analyses

During cruise SO-175, pore water analyses were carried out on selected gravity cores taken. From the MPF area, these included GeoB9006-1 and 9091-1 (Kopf et al. 2004). After coring the sediments were stored at a temperature of about 5°C. After splitting, sections of the core were squeezed using pressure filtration up to 5 bar. Afterwards the pore water was retrieved through through 0.2m cellulose acetate membrane filters. Different methods were used for these analyses. Alkalinity was measured by titration (Ivanenkov & Lyakhin 1978), silicate, phosphate and ammonium by spectro-photometry (Grasshoff et al. 1997). Pore waters were then analysed for major nutrients, total alkalinity, chloride, hydrogen sulphide, and methane (Kopf et al., 2004). In this paper, we only present a portion of the data, e.g. alkalinity, silicate, phosphate, and ammonium, since those are most indicative.

Results

Physical properties from MST and measurements on discrete samples

In Figure 4 we present some of the data from MST logging of the cores as well as water content and mean grain size from measurements on discrete samples. It can be seen that cores GeoB 9093-1 and GeoB 9092-1 from the middle portion of the landslide body are relatively homogeneous in their physical properties. As expected, the water content decreases quickly within the uppermost decimetres (from 50 to 40 %; Fig. 4A), and shows a moderate decrease below. Density remains near constant at ca. 1.6 g/cm^3. In contrast, both the headwall core (GeoB9008-2) and the most distal landslide tongue (GeoB 9091-1) show deviations in the physical properties curves.
Despite some overall downhole decrease in water content,

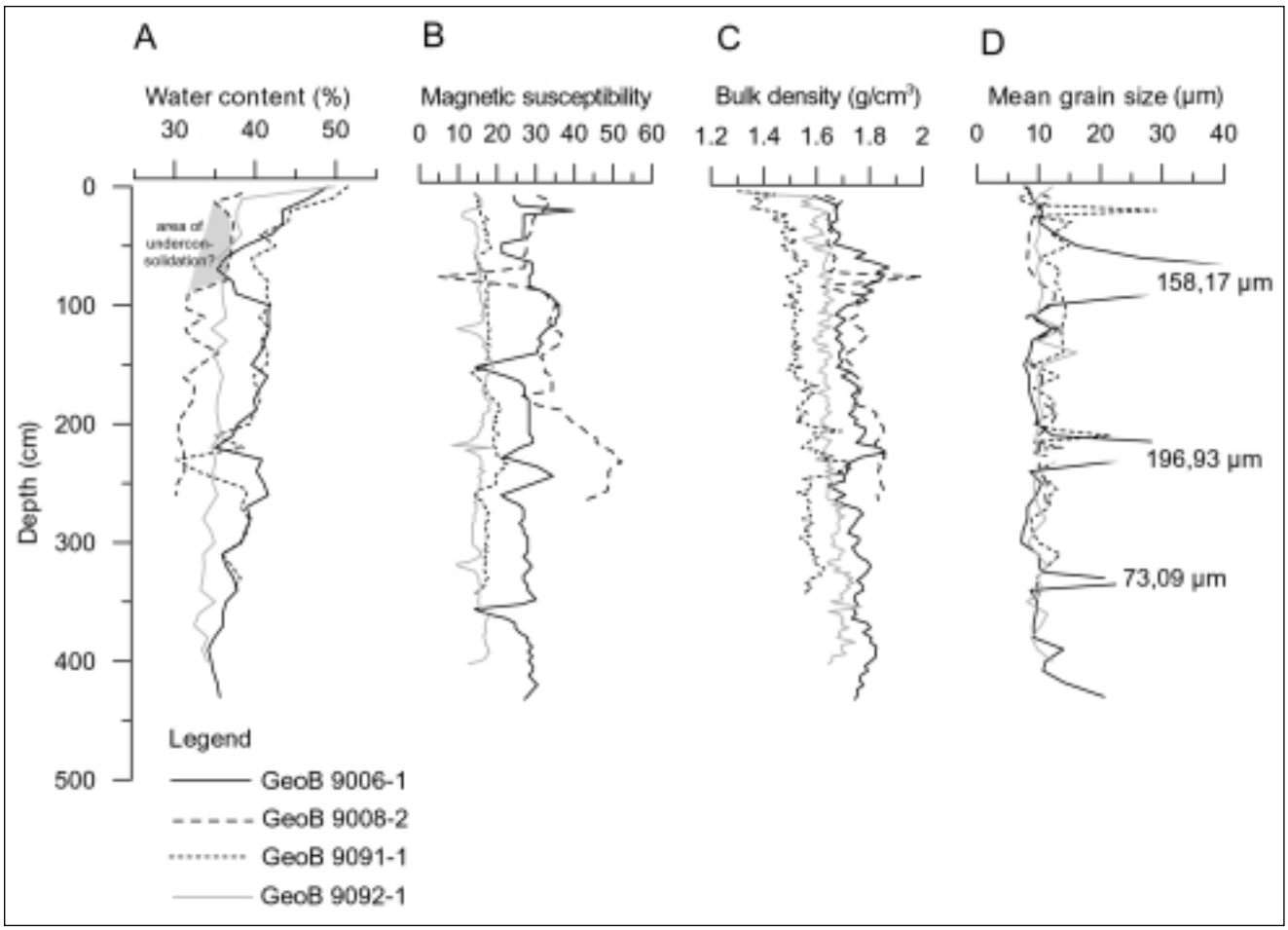

Fig 4: Physical properties of the five cores GeoB 9006-1. GeoB 9008-2, GeoB 9091-1, and GeoB 9092-1 from the MPF landslide area. A) Water content, B) bulk density, C) magnetic susceptibility, D) mean grain size. See text for discussion.

and increase in density in core GeoB 9008-2, there is one interval at the top that shows unusually high porosity (0 – 85 cm below sea floor [bsf]). The lower boundary of that interval shows peaks in bulk density up to ca. 2 g/cm^3 and mean grain size, which are accompanied by a minimum in magnetic susceptibility (Fig. 4B-D). This may mean that the initial landslide detachment surface is covered by about 85 cm of sediment fall after the event, with more sand-rich, non-magnetic deposits at the base. The material is less strongly consolidated than its footwall clays (Fig. 4A).

At the outermost tongue of the landslide, core GeoB 9091-1 shows a somewhat higher variability in physical properties. Density increases steadily down to ca. 225 cm bsf, and then drops back to 1.6 g/cm^3 (Fig. 4B). Mean grain size also shows the most profound spike just above 225 cm, suggesting a depositional change.

GeoB 9006-1, the reference core from outside the landslide area, shows an overall downhole decay in water content and porosity and a slight increase in bulk density. However, three clear peaks in mean grain size and water content are observed, which correspond to individual turbidite layers with a clear fining upward trend in grain size. These turbidites were mobilised somewhere on the Portuguese margin, very likely the Marquês de Pombal Mountain (Fig. 1), and then travelled westward onto the adjacent abyssal plain.

The undrained shear strength, as calculated from the falling cone tests (Hansbo 1957), shows an increase in shear strength with depth for all cores studied (Fig. 5). In summary, the mean undrained shear strength from the individual cores varies between 12,6 kPa (GeoB 9006-1) and 46,1 kPa (GeoB 9008-2) and decreases downslope. The range of undrained shear strength in the individual cores varies between 27,4 (GeoB 9006-1) and 97,9 (GeoB 9008-2) and also decreases downslope from headwall to tongue. However, there are differences in the absolute values and trends of the graphs.

The reference core GeoB 9006-1 shows a linear increase in strength, with < 30 kPa at the terminal depth of 420 cm bsf (Fig. 5). The two cores on the landslide's southern flow (Fig. 2) show similar linear trends, although the overall gradient is somewhat steeper (ca. 60 kPa [GeoB 9092-1] and 70 kPa [GeoB 9093-1], respectively). GeoB 9008-2 at the headwall of the MPF landslide exhibits the highest mean undrained shear strength, and also the widest range of shear

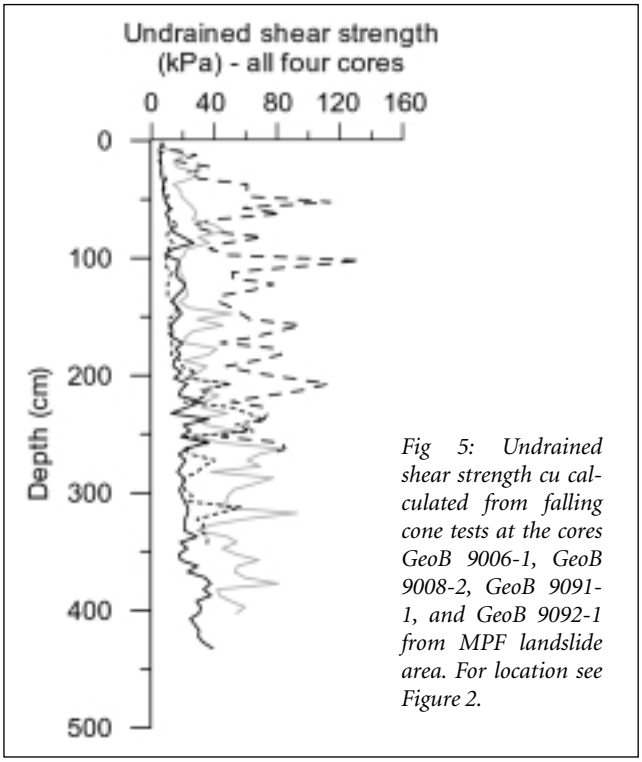

Fig 5: Undrained shear strength cu calculated from falling cone tests at the cores GeoB 9006-1, GeoB 9008-2, GeoB 9091-1, and GeoB 9092-1 from MPF landslide area. For location see Figure 2.

strength when compared with the other four cores. While the uppermost ca. 50 cm show strengths < 40kPa, the lower portion of that core scatters between c_u values of 30 kPa and 100 kPa (Fig. 5). Similar to the water content data, this leads us to suggest that the lower section at GeoB 9008-2 is overconsolidated (see discussion in Chapter 5 below).

At the most distal tongue of the landslide (GeoB 9091-1), variations in strength are near linear to a depth of around 200 cm bsf, where c_u is as low as 20 kPa (Fig. 5). Between 210 and 240 cm bsf, values start scattering, with an upper limit of about 50 kPa. At this depth, density, mean grain size and magnetic susceptibility also showed considerable scatter, the origin of which may be due to changes in deposition (see discussion below).

Grain size analyses and ring shear testing

The sampling strategy for the ring shear experiments was based on the earlier results from MST, core description, and physical properties measurements (see above). We measured one sample from the head scarp (core GeoB 9008-2) near the sediment surface at a depth of 6 cm bsf. Another sample was taken from the slide body of the southern flow (core GeoB 9093-1), in a depth of 260 cm bsf. A representative sample was selected, because the core is relatively homogeneous with respect to its physical properties (Table 2a). From core GeoB 9091-1, which is found to be the most diverse (see Figs. 4 and 5), a total of seven samples were tested in the ring shear device. As seen in the physical properties, we have a separation into two sediment packages with a transition at approximately 220 - 240 cm bsf. We took three samples from the upper part of the core (20 cm, 110 cm, 190 cm), two samples near the proposed boundary (225 cm, 240 cm), and two samples from the underlying sediment (280 cm, 345 cm). One sample was taken from reference core GeoB 9006-1 (234 cm) next to the landslide area.

With five of the samples (GeoB 9008-2_6 cm, GeoB 9093-1_260 cm, GeoB 9091-1_190 cm and _280 cm, and GeoB 9006-1_234 cm), we started the tests with a normal stress of 0,25 MPa and increased the normal stress incrementally up to a maximum of 16 MPa. These normal stress levels were chosen to submit the sediment to different conditions, but mostly to get more reliable results with respect to the rate-dependent frictional strength (see discussion in Marone, 1998). With the remaining five samples, all from core GeoB 9091-1 (20 cm, 110 cm, 225 cm, 240 cm, and 345 cm), we only went to normal stresses of 4 MPa, still sticking to the three different sliding velocities.

Table 2 summarises the results from the ring shear tests, falling cone tests, and grain size analyses. For the latter, please also refer to Figures 4 and 6. The ring shear tests showed mostly coefficients of friction between 0,21 and 0,29, which are typical for silty clays (e.g. Lupini et al., 1981; Brown et al., 2003). Residual strengths at 4 MPa normal stress and a sliding velocity of 0,03 mm/min varied between 0,8 and 1,4 MPa (Table 2). The lowest coefficient of friction and residual strength have been measured in core GeoB 9008-2 (6 cm) at the head scarp and GeoB 9091-1 (110 cm) in the redeposited lobe of the landslide (Table 2). When we plot the grain size classes of the distal core GeoB9091-1 versus depth, it can be seen that peaks in sand content correspond to an increase in density and c_u (Figs. 6, 7). If on the other hand clay content is plotted against friction coefficient (Fig. 7), abundant clay causes μ to drop, and vice versa.

The velocity stepping tests provided us with interesting results regarding the frictional sliding stability of the sediment (assuming this material acts as the detachment plane on an unstable slope). For the specimens tested in the ring shear apparatus, the calculated [a-b]-value ranges between -0,033 and 0,031 (Table 2). The majority of the analysed sediments show [a-b]-values very close to zero (+/- 0,005). The lowest [a-b]-value with -0,033 has been calculated for 240 cm in GeoB 9091-1. Also, the highest [a-b]-value with 0,031 has been found in GeoB 9091-1, right at the boundary between the remobilised portion of the landslide deposits and the underlying background sediments (225 cm). We address these data in the discussion (see below).

Pore water geochemistry

Table 2a. Results of ring shear tests in comparison to clay, silt, and sand contents of cores

	GeoB 9006-1 234 cm	GeoB 9091-13 20-345 cm	GeoB 9093-1 260 cm	GeoB 9008-2 6 cm
clay content (%)	25,6	21,9-25,0	22,4	22,8
silt content (%)	73,3	67,5-75,7	75,0	77,9
sand content (%)	1,1	0,7-10,7	2,6	0,3
res. shear strength (MPa)[1]	1,29	0,64-1,27	1,042	0,916
coeff. of friction[1]	0,258	0,158-0,31	0,257	0,226
[a-b]-value[2]	-0,017	-0,033-0,031	-0,003	0,021
Undrained shear strength (kPa, fall-cone tests)		2,21-40,73	20,16	7,02

[1] Measurements with 4 MPa normal stress and 0,03 mm/min slip velocity; Sample GeoB 9006-1, 234 cm with 5 MPa normal stress.
[2] as reviewed by Scholz, 1998.
[3] see also Table 2b

Table 2a: Results of ring shear tests in comparison to clay, silt, and sand contents of cores GeoB 9008-2, GeoB 9006-1, GeoB 9091-1 and GeoB 9093-1. Please note that results from grain size analyses are also shown in Figure 6.

Table 2b. Detailed results of core GeoB 9091-1 of the ring

GeoB 9091-1	20 cm	110 cm	190 cm	225 cm	240 cm	280 cm	345 cm
clay content (%)	21,7	25,0	24,5	22,7	23,8	25,9	23,3
silt content (%)	67,5	70,7	72,4	74,2	75,4	73,4	75,7
sand content (%)	10,7	4,3	3,2	3,1	0,7	0,8	0,9
res. shear strength (MPa)	1,029	0,64	0,91	1,27	0,996	0,83	1,088
coeff. of friction	0,254	0,158	0,224	0,31	0,246	0,204	0,268
[a-b]-value	-0,001	-0,004	0,01	0,031	-0,033	0,001	0,005
Undrained shear strength (kPa, fall-cone tests)	2,21	7,25	12,74	38,61	40,73	20,66	25,81

Table 2b: Detailed results of core GeoB 9091-1 of the ring shear tests in comparison to the clay, silt, and sand contents.

Owing to time constraints and the need to preserve some of the core for other research, only two of the five cores in the MPF landslide area were examined for pore water geochemical composition on board RV Sonne (Kopf et al., 2004). These were the GeoB9006-1 reference site as well as the GeoB9091-1 distal landslide site (Fig. 2).

The reference core showed quasi-linear trends in alkalinity or NH_4^+. In contrast, core GeoB 9091-1 pore water analyses show an abrupt change within the lower part of the core for most constituents (Fig. 8). Above 250 cm bsf alkalinity ranges between around 3.1 and 6.0 meq/l. Below 250 cm bsf alkalinity changes abruptly and is clearly higher with values between 7.0 and 10.0 meq/l. Similarly, the silica profile shows an abrupt change in a core depth around 220-250 cm bsf. Above 220 cm the concentration ranges between 100 and 130 µmol/l and below 220 cm Si concentration ranges between 150 and 200 µmol/l. The reference core does not show that bipolar trend in Si, but is characterised by a systematic downhole increase (some scatter included). While the upper part (0-150 cm bsf) ranges from 90 – 110 µmol/l, the middle part (150 – 250 cm bsf) ranges from 120 – 150 µmol/l, and Si in the lower portion (250 – 410 cm bsf) plots between 170 and 200 µmol/l. We attribute the distinct change in pore water chemistry to the observations of variable physical properties in that interval (see Chapter 4.1), most likely related to some change in deposition.

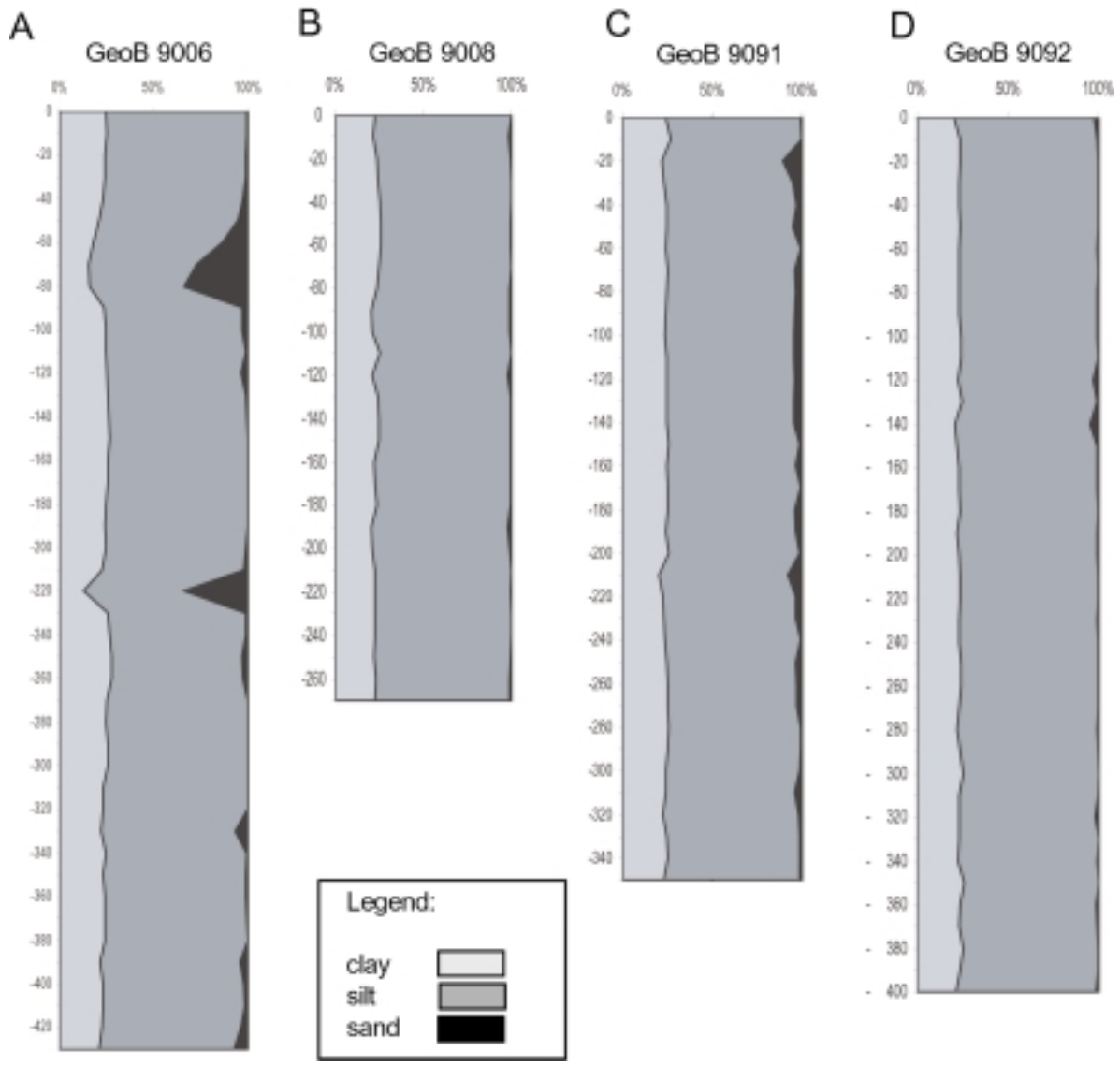

Fig 6: Grain size distribution of cores GeoB 9006-1, GeoB 9008-2, GeoB 9091-1, and GeoB 9092-1 from MPF landslide area. For location see Figure 2.

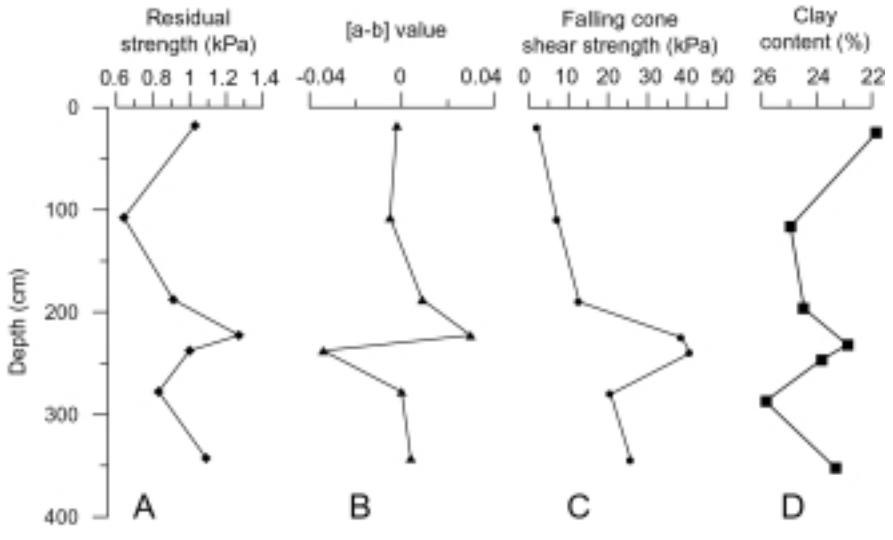

Fig 7: Results from ring shear tests on specimens taken fron core GeoB 9091-1. A) Residual shear strength, B) [a-b] value. For comparison, clay content (C) and undrained shear strength from falling cone tests (D) are also given. See text.

Discussion

The pore water analyses of GeoB 9091-1 show an interesting change at a core depth around 220 - 250 cm (Fig. 7). This change, which is most obvious for the alkalinity and Si profiles, suggests that pore waters in the upper and lower portion of the core are not in equilibrium. Earlier work has attested that pore water chemistry is a powerful proxy in dating turbidite events and submarine landslides (Zabel & Schulz 2001). In addition to the geochemistry of the fluids, most of the physical properties such as density, water content or undrained shear strength also show profound variations in the interval between 220 and 240 cm (Figs. 4, 5, 7). Such characteristics are in favour of a zone of instability, i.e. a discontinuity in the sedimentary succession. When combined, our results suggest that we have two different units in GeoB 9091-1 with the boundary between them at approximately 220 - 250 cm. It also means that the upper unit comprises deposits remobilised from the landslide further upward on the Marquês de Pombal Mountain, while the lower unit consists of the regional background sediment.

In the discussion we will focus on two main aspects. First, we will address the physical properties of the landslide deposits, namely the rate-dependent frictional behaviour and its implications for slope stability. Second, we will use our geochemical data to model deposition of the distal sediments penetrated at GeoB9091-1, and tie them into the regional framework of potential triggers of the landslide and subsequent turbidites.

Frictional stability of the MPF landslide deposits

One of the main parameters influencing the stability of submarine slopes is the low intrinsic frictional strength of clay minerals, especially when water-saturated (e.g., Lupini et al. 1981; Logan & Rauenzahn 1987; Brown et al. 2003). In fact, slopes being (partly) covered in such sedimentary sequences do not require much of a trigger before failure occurs. For this reason, we here discuss the results from ring shear testing of seawater-saturated sediments in the light of intrinsic strength. Figure 9 plots the projected positions of the five sediment cores from the landslide area onto seismic reflection profile (station GeoB 9094-2) acquired in E-W direction across the landslide (Kopf et al. 2004). Insets show how to calculate the [a-b]-value as well as the [a-b]-values calculated from our ring shear results. While the majority of the [a-b]-values are very close to zero, three specimens are different: GeoB 9091-1_225 cm with μ=0,031, GeoB 9091-1_240 cm with μ=-0,033, and GeoB 9008-2_6 cm with μ=0,021. Most importantly, both sediments taken at the head scarp (GeoB 9008-2) and at the very toe of the slide show distinct positive [a-b]-values and thus, velocity strengthening behaviour. Materials showing velocity strengthening tend to produce inherently stable frictional slip; when water-saturated, the majority of the clay minerals fall into this group. We tentatively conclude here that weak layers within our gravity cores in the MPF landslide region show velocity strengthening and are hence predestined to fail. In contrast to those observations, GeoB 9091-1_240 cm shows velocity weakening. Here the shear strength decreases with increased rate, potentially causing either unstable stick-slip or only conditionally stable behaviour (e.g. Scholz 1998; Saffer & Marone 2003).

A reason for the similarity of GeoB 9008-2 (6 cm) and GeoB 9091-1 (225 cm) might be that, in both cases, we regard supposed failure planes. Near the head scarp subbottom deposits, as well as at the boundary between the upper and lower unit, one anticipates weak material properties and stable frictional sliding behaviour. This is exactly what our ring shear results attest (Figs. 7, 9). Figure 7 further illustrates the near perfect match of the strength from the falling cone and ring shear tests with the [a-b] data. With respect to post-slope failure dynamics, these results further imply that runout distances may be very high. If we now relate this finding to the estimated length (i.e. 24 km) and sediment volume (1.3 km^3) of the slide (see Gràcia et al. this volume; Vizcaino et al. this volume), our data agree well with the results by those workers.

Timing and triggering of the distal mass wasting deposit

Based on the strong deviation of most of our geochemical signatures in the pore waters of core GeoB 9091-1 (Fig. 8), we conclude that the uppermost 220 - 250 cm of the sediments were out of equilibrium with their footwall deposits. When modelling emplacement and allowing for diffuse flow with time, we can allocate certain fits to the geochemical deviations in the core. For a detailed description of the modelling method refer to Hensen et al. (1997), or Hensen et al. (2003). Figure 10A shows the modelling results and the measured data points of the silicate concentrations in the pore waters. The small black line shows the assumed situation at the time of our small mass movement event. The thicker black line shows the modelled situations after 5 years, the dark grey line the situation after 10 years and the lighter grey line shows the modelled situation after 20 years. It can be seen that the longer diffusion is allowed, the more anticipated pore water composition deviates from the actual shipboard data (Kopf et al., 2004). Consequently, we propose that deposition must have taken place around five years prior to sampling in late 2003. It should be noted, however, that the diffusion modelling has to be treated with some caution since it requires a distinct boundary to be picked between the hangingwall and footwall sedimentary package. In the case of the

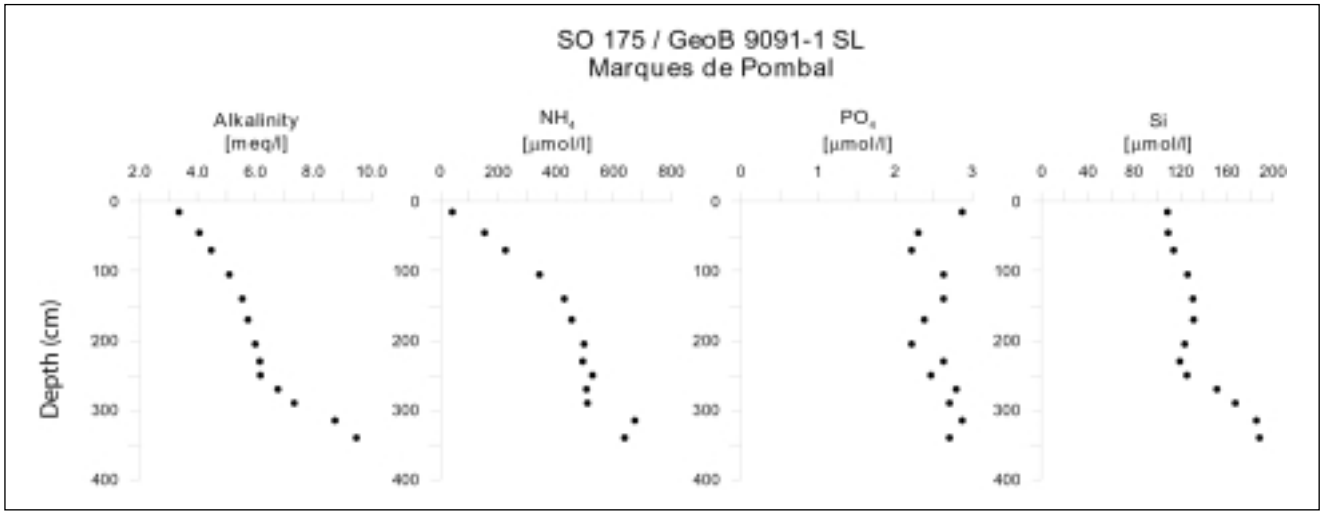

Fig 8: Pore water geochemical data from gravity core GeoB 9091-1 from the most distal portion of the Marques de Pombal landslide: (A) Alkalinity, (B) NH4, (C) PO4, and (D) Si.

upper unit, however, such a boundary cannot be picked from core observation without some uncertainty (see Fig. 8). In fact, the macroscopic homogeneity of the sediments of that core suggests that some of the background sediments got amalgamated into the slid upper unit. Still, pore water chemistry attests an individual redepositional event that matches our modelled curves (Fig. 10A).

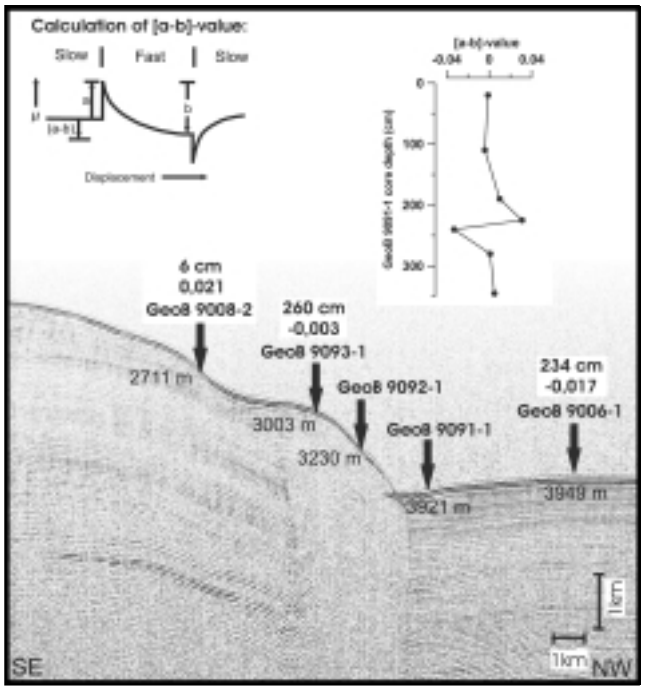

Fig 9: Schematically positions of the five cores from the landslide area projected into the seismic line (GeoB 9094-2, Kopf et al. 2004) across the slope. The profile length is approximately 21 km (Kopf et al. 2004); for location refer to Figure 2 Included are the [a-b]-values calculated from the ring shear tests after Scholz (1998). In the top left-hand corner of the diagram is shown how to calculate the [a-b]-value after review by Scholz (1998).

An important question for slope stability analyses is always what mechanism initiates a submarine slide. Before discussing the potential trigger mechanism(s), it should be pointed out that the event we have dated is not contemporary with the emplacement of the MPF slide (see Vizcaino et al., this volume). In fact, quite the opposite is the case. While the main sliding event can be narrowed down to having been triggered some 3000 years ago, some of the then slid deposits may have temporarily ended up in a metastable position on the Portuguese slope. Consequently, a fairly minor variation in physical condition may have caused these deposits to slide some five years ago. This may include earthquake tremor, oversteepening of the slope caused by tectonic displacements along the MPF (i.e. readjustment to critical taper), fluid migration, or even tidal loading.

We have investigated the various regional records at the time. The only hint towards natural hazards being possibly associated with the emplacement of the 220-250 cm-thick mass wasting deposit at the distal slide body is an earthquake some 120 km away to the NE (Fig. 10B). According to Malamud et al. (2004), earthquake tremor of M4.3 is required to trigger a landslide. When compiling seismic records in the time window envisaged (i.e. 5 years prior to the cruise SO175), the only significant earthquake near the study area coincidentally was a M4.3 tremor some 120 km NE of the MPF slide. It is not certain that this rather distant event has affected the MPF area, however, no other obvious process has been recorded. Still, sliding may have simply occurred due to other processes such as vertical loading (due to tidal, tectonic or sedimentary reasons), etc. even progressive sedimentation, causing increasing shear stresses on the clays at the basal interface of the landslide (headwall and ca. 225 cm-deep distal lobe) may have been a trigger sufficient for sliding given the low overall frictional strength.

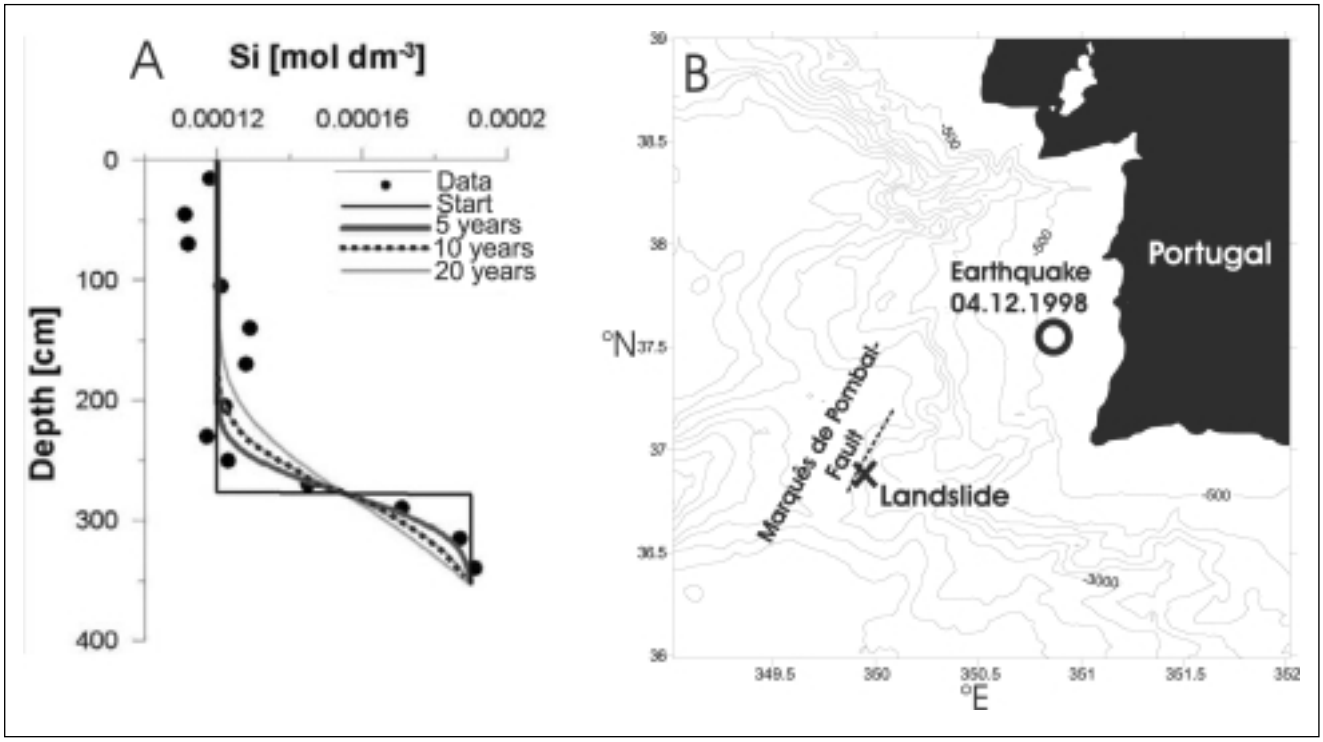

Fig 10: A) Si concentrations in GeoB 9091-1 pore waters and modelled trends simulating emplacement of the uppermost 225 cm-thick sediment package at 5, 10, and 20 yrs. before sampling. B) Location of the Marques de Pombal landslide and location of an earthquake from 1998.

Conclusions

In conclusion, the ring shear results show a general velocity weakening behaviour of the landslide sediments. The only exception to this are the silty clays at the supposed failure planes along the landslide (GeoB 9008-2 beneath the headwall of the slide) and the small mass movement event at the distal lobe (GeoB 9091-1). The low strength and velocity strengthening (i.e. stable sliding) behaviour are indicative that low intrinsic strength may have required only a small external trigger before slope failure occurred. It further implies that post-failure mass wasting is characterised by large runout distances. Both of these results are supported by independent evidence. As for the trigger, a nearby M4.3 earthquake supports the idea that not much stress change was required to trigger sediment remobilisation in the frontal portion of the southern MPF landslide. As for the overall geometry of both the northern and southern flow, our geotechnical data agree well with the large runout length and small thickness of the landslide.

Acknowledgements. We thank Eulalia Gràcia for sharing a backscatter image and other valuable geophysical data in the working area, without which our coring programme had been less successful. We also thank Kristin Nass for helping with the pore water analyses on board R/V Sonne. Finally we thank BMBF and DFG for supporting the cruise and follow-up research, respectively. This is RCOM publication #0420.

References

Argus, D.F., Gordon, R.G., DeMets, C. & Stein, S. 1989: Closure of the Africa-Eurasia-North America plate motion circuit and tectonics of the Gloria fault. *Journal of Geophysical Research* 94, 5585-5602.

Bishop, A.W., Green, G.E., Garga, V.K., Andresen, A. & Browns, J.D. 1971: A new ring shear apparatus and its application to the measurements of residual strengths. *Géotechnique* 21, 273-328.

Brown, K.M., Kopf, A., Underwood, M., Steurer, J. & Weinberger J.L. 2003: Frictional and mineralogic properties of sediments entering the western Nankai subduction zone: Implications for state of stress on the subduction thrust. *Earth and Planetary Science Letters* 214, 589-613.

Gràcia, E., Danobeitia, J.J., Verges, J., PARSIFAL Team 2003: Mapping active faults offshore Portugal (36°N-38°N): Implications for seismic hazard assessment along the southwest Iberian margin. *Geology* 31, 83-86.

Grasshoff, K., Ehrhardt, M. & Kremling, K. 1997: *Methods of seawater analysis.* Verlag Chemie.

Gutscher, M.A., 2004. What Caused the Great Lisbon Earthquake? *Science* 305, 1247-1248.

Hansbo, S. 1957. A new approach to the determination of the shear strength of clay by the fall-cone test. Geotechnical Institute Proceedings no. 14, Stockholm 1957, p 50.

Head, H.K. 1994: Manuel of Soil Laboratory Testing, Volume 2: Permeability, Shear Strength and Compressibility Tests. Second Edition. New York, Toronto. 433pp.

Hensen, C., Landenberger, H., Zabel, M., Gundersen, J.K., Glud, R.N. & Schulz, H.D. 1997: Simulation of early diagenetic proceses in continental slope sediments off southwest Africa: the computer model CoTAM tested. *Marine Geology* 144, 191-210.

Hensen, C., Zabel, M., Pfeifer, K., Schwenk, T., Kasten, S., Riedinger, N., Schulz, H.D. & Boetius, A. 2003: Control of sulfate pore water profiles by sedimentary events and the significance of anaerobic

oxidation of methane for the burial of sulphur in marine sediments. *Geochim. Cosmochim. Acta* 67, 2631-2647.

Ivanenkov, V. N. and Lyakhin, Y. I. 1978. Determination of total alkalinity in seawater. *In* Bordovsky, O.K. & Ivenenkov, V. N. (eds.), *Methods of hydrochemical investigations in the ocean*. Nauka Publ. House, Moscow, 110-114

Kopf, A., Bannert, B., Brückmann, W., Dorschel, B., Foubert, A.T.G., Grevemeyer, I., Gutscher, M.-A., Hebbeln, D., Heesemann, B., Hensen, C., Kaul, N.E., Lutz, M., Magalhaes, V.H., Marquardt, M.J., Marti, A.V., Nass, K.S., Neubert, N., Niemann, H., Nuzzo, M., Poort, J.P.D., Rosiak, U.D., Sahling, H., Schneider von Deimling, J., Somoza Losada, L., Thiebot, E., Wilkop, T.P. 2004: GAP cruise report: Gibraltar Arc Processes, FS *Sonne* SO175, Berichte der Geowissenschaften, Univ. Bremen 228, 218pp.

Kopf, A. & Brown, K.M. 2003: Friction experiments on saturated sediments and their implications for the stress state of the Nankai and Barbados subduction thrusts. *Marine Geology* 202, 193-210.

Logan, J.M. & Rauenzahn, K.A., 1987: Frictional dependence of gouge mixtures of quartz and montmorillonite on velocity, composition and fabric. *Tectonophysics* 144, 87-108.

Lupini, J.F., Skinner, A. & Vaughan, A.E. 1981: The drained residual strength of cohesive soils. *Géotechnique* 31, 181-213.

Malamud, B.D., Turcotte, D.L., Guzzetti, F. & Reichenbach, P. 2004: Landslides, earthquakes, and erosion. *Earth and Planetary Science Letters* 229, 45-59.

Marone, C.J. 1998: Laboratory-derived friction laws and their application to seismic faulting. *Annual Reviews Earth Planetary Science* 26, 643-696.

Mienert, J., Berndt, C., Laberg, J.S. & Vorren, T.O. 2003: Slope Instability of Continental Margins. *In* Wefer et al. (Eds.), *Ocean Margin Systems, Springer Verlag, New York,* 179-193.

Normenausschuss Bauwesen (NABau) im DIN Deutsches Institut für Normung e.V., 1990: DIN 18 137 Teil 1: Baugrund, Versuche und Versuchsgeräte – Bestimmung der Scherfestigkeit, Begriffe und grundsätzliche Versuchsbedingungen, 320-333.

Saffer, D.M. & Marone, C. 2003: Comparison of smectite- and illite-rich gouge frictional properties: application to the updip limit of the seismogenic zone along subduction megathrusts. *Earthquake and Planetary Science Letters* 215, 219-235.

Sartori, R., Torelli, L., Zitellini, N., Peis, D. & Lodolo, E. 1994: Eastern Segment of the Azores-Gibraltar Line (Central-eastern Atlantic): An Oceanic Plate Boundary with Diffuse Compressional Deformation, *Geology* 22, 555-558.

Scholz, C.H., 1998: Earthquakes and friction laws. *Nature* 391, 37-42.

Wood, D.M. 1985: Some fall-cone tests. *Geotechnique* 35, 64-68.

Zabel, M., & Schulz, H.D. 2001: Importance of submarine landslides for non-steady state conditions in pore water systems – lower Zaire (Congo) deep-sea fan. *Marine Geology* 176, 87-99.

Zitellini, N., Rovere, M., Terrinha, P., Chierici, F., Matias, L. & Bigset Team 2004: Neogene Through Quaternary Tectonic Reactivation of SW Iberian Passive Margin. *Pure Applied Geophysics* 161, 565-587.